

Charge transfer and electronic screening at the As/Si(100)-(2×1) and As/Si(111)-(1×1) surfaces

R. J. Cole, J. A. Evans, and P. Weightman

*Department of Physics and Surface Science Research Centre, University of Liverpool,
Liverpool L69 3BX, United Kingdom*

J. A. D. Matthew

Department of Physics, University of York, Heslington, York YO1 5DD, United Kingdom

D. A. Woolf and D. I. Westwood

Department of Physics, University College of Wales, Cardiff, United Kingdom
(Received 5 October 1993; revised manuscript received 19 November 1993)

As and Si Auger parameters for As terminated Si(100) and Si(111) surfaces have been measured and analyzed in terms of ground state charge transfer across the interfaces and core hole screening efficiency. Our results indicate a small electron transfer (~ 0.05 electrons per atom) from Si to As at these interfaces. We find that for the As/Si(100) system core holes in atoms in the interface layers are much better screened than in bulk Si, due to high polarizability in the As-As bond. The screening is more bulklike at the As terminated Si(111) surface, consistent with the unreconstructed "bulk-terminated" surface structure of this system.

I. INTRODUCTION

Arsenic termination of Si surfaces yields very low energy and chemically passivated surfaces that can be used to manipulate epitaxial growth modes.^{1,2} As on Si systems also features in attempts to integrate GaAs and Si semiconductor technology.^{3,4} The study of the charge transfer and relaxation energy shifts at semiconductor surfaces and interfaces is now attracting increasing interest.^{5,6}

In our earlier work,⁶ Auger parameter (AP) shifts for the As terminated Si(100) surface with respect to the bulk elemental solids were reported. In the present work the measurements are repeated for the As/Si(111)-(1×1) system, and AP shifts for both systems are interpreted in terms of ground state charge transfer and the local dielectric properties of the interfaces.

II. EXPERIMENT

As/Si(111) samples were grown on a *p*-type (0.75–1.25 Ω cm B-doped) Si substrate using a VG Semicon V80H molecular beam epitaxy (MBE) reactor. The Si wafer was HF etched followed by an HCl:H₂O₂:H₂O (1:7:1) reoxidation routine⁷ and then introduced into the MBE reactor. The oxide layer was desorbed by annealing at $\sim 850^\circ\text{C}$ for 30 min, after which the substrate was allowed to cool to 120°C in an incident As₄ flux of $\sim 5 \times 10^{14}$ molecules cm⁻² s⁻¹. Following the epitaxial growth of an As monolayer, the specimen was held at low temperature ($< 15^\circ\text{C}$) in the As₄ flux for about 1 h. Post-growth reflection high energy electron diffraction (RHEED) observations suggested the As overlayer to be

amorphous in nature. Deposition of this cap provided a protective layer for the underlying As/Si interface, allowing removal of the specimens from the MBE apparatus and transfer into analysis spectrometers without exposing the interface. In addition, the cap allowed the measurement of core level photoelectron and core-core-core Auger electron energies for bulk As.

A sample was transferred to an electron spectrometer⁸ and the As cap was cleaned by resistive heating to $\sim 300^\circ\text{C}$ for periods of a few seconds. As *L*₃*M*₄₅*M*₄₅ Auger spectra were excited using x rays from an Mo anode, operating the electron analyzer in fixed transmission mode at a resolution of 0.07 eV. Photoelectron spectra obtained using a monochromated Al x-ray source with 0.5 eV resolution were also recorded. No Auger or photoelectron lines were observed from the Si substrate which, considering electron escape depths,⁹ indicates a cap thickness greater than $\sim 200 \text{ \AA}$.

The As cap was then desorbed by heating to 400°C for 60 min, leaving only the As monolayer termination of the Si(111) surface. Scanning tunneling microscopy studies¹⁰ have shown this procedure to produce an atomically smooth As termination of the Si(111) surface. A very sharp characteristic 1×1 low energy electron diffraction pattern was observed, and x-ray photoelectron spectroscopy (XPS) showed the specimen surface to be free of contamination. The 2*p* photoelectron spectra of Si and As and the As *L*₃*M*₄₅*M*₄₅ and Si *K**L*₂₃*L*₂₃ Auger spectra of the As terminated Si(111) surface were then measured. Although the Si spectra contain contributions from both the interface and bulk sites, the large escape depth [$> 25 \text{ \AA}$ (Ref. 9)] for the *KLL* Auger electrons causes the bulk component to dominate. In order to enhance the interface signal and subsequently allow separation of bulk and

interface contributions, Si *KLL* spectra were taken using eight different electron emission angles θ , ranging from 0° to 70° from the surface normal.

III. RESULTS

A. Arsenic spectra

Comparison of the As valence band photoelectron spectrum with the work of Ley *et al.*¹¹ suggested the capping layer to be amorphous in nature. This conclusion is in agreement with the post-growth RHEED observations and with the results of Raman spectroscopy performed on identical specimens.¹²

The As $2p_{3/2}$ photoelectron and $L_3M_{45}M_{45}$ Auger spectra of the cap and the As/Si(111)-(1 \times 1) system are shown in Figs. 1(a) and 1(b), respectively, and the photoelectron and Auger chemical shifts are tabulated in Table I.

B. Silicon spectra

Using synchrotron radiation, Olmstead *et al.*¹³ have obtained a surface sensitive and high resolution (0.3 eV) Si $2p$ spectrum of the As/Si(111) system which shows an interface component 0.75 ± 0.01 eV more bound than the bulk contribution. The corresponding Si $KL_{23}L_{23}^1D_2$ spectrum for $\theta = 0^\circ$ (normal emission) is shown by the crosses in Fig. 2. To establish the presence of a chemically shifted Auger interface component we first sought to fit this spectrum to a single Lorentzian. This produced the simulated curve shown by the solid line in Fig. 2 with peak position 1611.54 eV. The fit is relatively poor and the Lorentzian width was required to be 1.10 eV, larger than the previously determined lifetime broadening of the bulk component.⁶ The discrepancy between the experimental data and the single component fit becomes progressively worse as θ is increased. This is clearly illustrated by the experimental spectrum for $\theta = 60^\circ$ plotted as circles in Fig. 2. We conclude that the Si $KL_{23}L_{23}$ spectrum includes an interface component with lower kinetic energy than that of the contribution from the bulk sites.

Assuming an exponential photocurrent attenuation with distance from the sample surface, the fractional intensity $I_s(\theta)$ derived from the Si interface layer is given by

$$I_s(\theta) = 1 - \exp\{-d/(\lambda \cos \theta)\}, \quad (1)$$

TABLE I. Measured arsenic chemical shifts ΔE_b and ΔE_k , and Auger parameter shifts $\Delta \xi$ and $\Delta \beta$ for As/Si(111)-(1 \times 1) and As/Si(100)-(2 \times 1) relative to bulk As. All measurements are in eV. The difference in work function between bulk As and the As terminated Si specimens introduces an additional uncertainty in the determination of $\Delta \beta$ as discussed in Sec. IV A.

System	$\Delta E_k(LMM)$	$\Delta E_b(2p)$	$\Delta \xi$	$\Delta \beta$
As/Si(111)	-0.60 ± 0.04	-0.40 ± 0.04	-0.94 ± 0.06	-1.80 ± 0.06
As/Si(100)	-0.52 ± 0.04	-0.12 ± 0.04	-0.62 ± 0.06	-0.88 ± 0.06

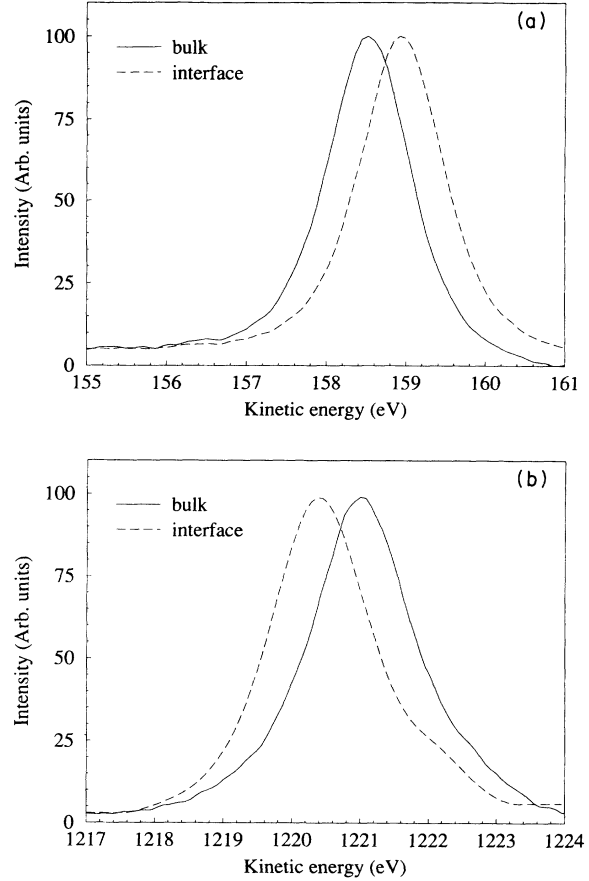


FIG. 1. (a) Arsenic $2p_{3/2}$ and (b) arsenic *LMM* Auger spectra of the As/Si(111) interface (dashed curve) and of bulk As (solid curve). The spectra in Figs. 1–3 are referenced to the spectrometer vacuum level.

where d is the thickness of the Si interface layer and λ is the electron escape depth. To facilitate the separation of bulk and interface Auger components we first used the Si $2p$ photoelectron spectrum with $\theta = 60^\circ$ obtained in the present work to determine d/λ . This spectrum was modeled using two spin-orbit split doublets, each consisting of two Lorentzians with lifetime broadening 0.08 eV,¹⁵ intensity ratio 2:1, and spin-orbit splitting 0.6 eV. Using the interface chemical shift determined by Olmstead *et al.*¹³ we found $I_s = 0.18$, and from Eq. (1) we obtained $d/\lambda = 0.10$.

Auger spectra for $\theta = 0^\circ, 10^\circ, 20^\circ, \dots, 70^\circ$ were then each modeled by two Lorentzian components each with a full width at half maximum of 1.0 eV.⁶ The eight spec-

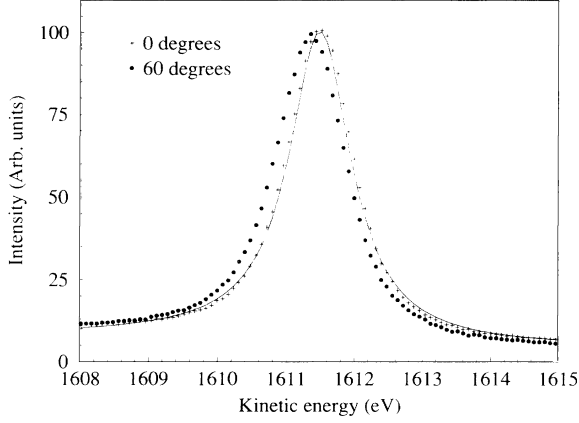


FIG. 2. Si $KL_{23}L_{23}:^1D_2$ spectra from the As/Si(111) interface for $\theta = 0^\circ$ (crosses) and 60° (circles). The solid curve is a numerical fit to the 0° spectrum using a single component.

tra were *simultaneously* fitted, constraining $I_s(\theta)$ according to Eq. (1) with $d/\lambda = 0.10$. In this procedure the only free parameters are the kinetic energy of the interface and bulk contributions. Optimum fits were obtained with bulk and interface components at 1611.59 and 1611.14 eV, respectively, as shown in Fig. 3. Since the escape depth for the Si KLL Auger electrons is expected to be⁹ $\sim 10\%$ greater than for $2p$ photoelectrons excited by 1487 eV photons, the fitting procedure was also performed with d/λ as a free parameter. Allowing d/λ to vary from 0.1 and the lifetime broadening to vary from 1.0 eV gave $\Delta E_k = 0.45 \pm 0.04$ eV with no significant improvement in the fit quality.

Although the interface component of the Si $KL_{23}L_{23}:^1D_2$ line is not resolved experimentally, this simultaneous fitting procedure in which the peak positions are the only free parameters imposes strict constraints on the line shape analysis. The success in fitting all eight spectra shows that ΔE_k given in Table II is reliably and accurately determined.

IV. DISCUSSION

We write the core potential V for an atom in some chemical environment as

$$V = V_{\text{core}} + kq + U, \quad (2)$$

where V_{core} is the contribution from the nucleus and the core electrons, q is the valence charge associated with

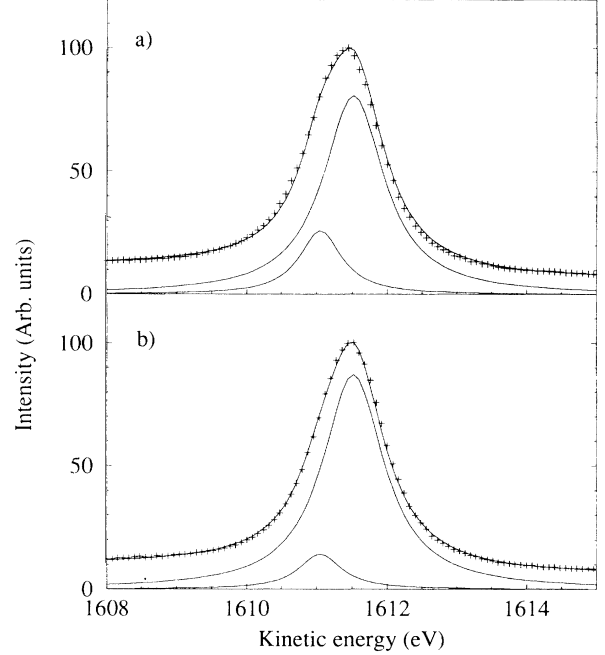


FIG. 3. Si $KL_{23}L_{23}:^1D_2$ spectra for (a) $\theta = 60^\circ$ and (b) $\theta = 20^\circ$. The experimental data are shown by crosses with the numerical fits given by the accompanying solid curves. Bulk and interface components are also shown.

the atom, k is the potential per valence charge, and U is the extra-atomic contribution. Shifts in core potential ΔV can then be related to ground state charge transfer Δq , although the experimental quantities ΔE_b and ΔE_k are determined by both ΔV and changes in the dynamic relaxation energy ΔR . We now consider initial and final state Auger parameter shifts, defined by

$$\Delta\beta = 3\Delta E_b + \Delta E_k \quad (3)$$

and

$$\Delta\alpha = \Delta E_b + \Delta E_k, \quad (4)$$

respectively.

A. Initial state Auger parameter

The initial state AP shift for an atom in two different chemical environments may be written¹⁶

$$\Delta\beta \approx 2\Delta q(k - M), \quad (5)$$

TABLE II. Measured silicon chemical shifts ΔE_b and ΔE_k , and Auger parameter shifts $\Delta\xi$ and $\Delta\beta$ for As/Si(111)-(1 \times 1) and As/Si(100)-(2 \times 1) relative to bulk Si. All measurements are in eV.

System	$\Delta E_k(KLL)$	$\Delta E_b(2p)$	$\Delta\xi$	$\Delta\beta$
As/Si(111)	-0.45 ± 0.04	0.75 ± 0.01^a	0.05 ± 0.04	1.80 ± 0.04
As/Si(100)	0.23 ± 0.04	0.45 ± 0.01^b	0.52 ± 0.04	1.58 ± 0.04

^aReference 13.

^bReference 14.

where M represents the Madelung potential. While $\Delta\beta$ provides a direct measurement of the ground state charge transfer, estimates of Δq determined from Eq. (5) may carry quite large errors for a number of reasons. First, Eq. (5) relies on the approximation that the relaxation energy for a two hole state is four times that for a one hole state and the assumption that all core levels suffer equal chemical shifts. Also k and M have similar magnitude so that modest uncertainties in determining k (Ref. 16) or M (due to relaxation of the atomic positions at the surface) lead to large errors in their difference. Finally, in measuring β the experimental errors can be large compared with $\Delta\beta$ since ΔE_b and ΔE_k must be accurately referenced. Nonetheless, we expect $\Delta\beta$ to provide a useful first approximation of Δq .

B. Final state Auger parameter

While to first order $\Delta\alpha$ is twice the change in dynamic relaxation energy, expanding XPS and Auger energies as Taylor series of V in core occupancy N , Thomas and Weightman¹⁶ have derived the expression

$$\Delta\alpha = \Delta \left\{ q \frac{dk}{dN} + \frac{dq}{dN} \left(k - 2 \frac{dk}{dN} \right) + \frac{dU}{dN} \right\}. \quad (6)$$

In metallic systems core hole screening is extremely local and (6) takes a particularly simple form in which only the first term is nonzero. AP shifts are therefore a direct measure of charge transfer in metals.¹⁶ In semiconductors the core hole screening efficiency is much reduced, and consequently AP shifts must be understood in terms of charge transfer screening (dq/dN) and polarization (dU/dN), as well as charge differences in the initial state.¹⁷⁻²⁰

Implicit in the derivation of Eq. (6) is the assumption that i, j, k , and l all experience the same potential shift due to changes in valence charge distribution. Chemical shifts of the $1s$ and $2p$ levels of Si atoms in a variety of environments can be found in the literature, and in general one finds that $\Delta E_b(1s) > \Delta E_b(2p)$.²¹ Sodhi and Cavell²² have noted that the ratio $\Delta E_b(j)/\Delta E_b(i)$ has a well defined value f , and compiling data from the literature Rivière *et al.*²¹ have found $f_{\text{Si}} = \Delta E_b(2p)/\Delta E_b(1s) = 0.74 \pm 0.02$ and $f_{\text{As}} = \Delta E_b(3d)/\Delta E_b(2p) = 0.93 \pm 0.01$. For this reason it is useful to consider the more general final state AP ξ of Lang and Williams,²³ given by

$$\begin{aligned} \xi(ijj) &= E_k(ijj) + 2E_b(j) - E_b(i) \\ &= E_k(ijj) + (2 - 1/f)E_b(j). \end{aligned} \quad (7)$$

Although the chemical shift of the Si $1s$ level at the As/Si interfaces could not be obtained experimentally, $\Delta\xi$ was obtained using the second equality in Eq. (7). Values of $\Delta\xi_{\text{As}}$ and $\Delta\xi_{\text{Si}}$ for the two As/Si systems are given in Tables I and II, respectively.

The difference in $\xi(ijj)$ between two chemical environments is given by

$$\Delta\xi(ijj) = \Delta \left\{ q \frac{dk(j)}{dN} + \frac{dq}{dN} \left(k(j) - 2 \frac{dk(j)}{dN} \right) + \frac{dU}{dN} \right\}, \quad (8)$$

which is equivalent to (6) provided that the k parameter appropriate to the shallower core level j is used. The evaluation of the atomic potential parameters k and dk/dN has been described at some length in earlier work^{6,16,17} and values have been obtained for As and Si.⁶ In this earlier work we found that k and dk/dN for Si are 11.5 and -3.3 eV, and for As are 11.2 and -2.8 eV, respectively.

It should also be noted that the final state AP's α and ξ are determined by spectral separations of Auger and XPS lines, rather than absolute Auger and photoelectron binding energies, and so are independent of reference energy.

V. ANALYSIS

A. Analysis of initial state AP shifts

Values of $\Delta\beta_{\text{Si}}$ for the Si interface layers at the As terminated surfaces are given in Table II. The Madelung terms were calculated by the Evjen method giving values of 8.3 and 5.7 eV for the top Si layer in the As/Si(111) and As/Si(100) structures, respectively. Application of Eq. (7) suggests the interface Si atoms have positive charges, losing 0.28 electrons per atom and 0.16 electrons per atom in the (111) and (100) systems, respectively. A similar quantitative analysis cannot be carried out for the As $\Delta\beta$ measurements since the spectra for bulk As and As on Si have different reference energies, and β is not a reference free quantity. Nevertheless, the sign of $\Delta\beta_{\text{As}}$ is consistent with a negative charge on As in both systems.

Despite the uncertainties in both measuring and analyzing the initial state AP shifts, our results unambiguously give the direction of electron transfer to be from Si to As at As terminated (111) and (100) surfaces.

B. Dielectric screening model of final state AP shifts

Here we adopt a simple dielectric screening model^{6,17} in which we consider an atom at the center of a spherical cavity embedded in a medium of dielectric constant ϵ . Equation (8) becomes¹⁷

$$\Delta\xi = \Delta q \frac{dk}{dN} - \Delta \left(\frac{1}{\epsilon} \right) \left\{ k - 2 \frac{dk}{dN} \right\}, \quad (9)$$

showing that in semiconducting systems dielectric differences can dominate $\Delta\xi$ — a positive value of $\Delta\xi$ indicating an increased screening efficiency, and a negative value a poorer screening environment. Although here we use the cavity model beyond its intended range of application, we find justification for this in the fact that for nonmetallic systems local polarization and screening ef-

fects are dominated by the nearest neighbors.¹⁹ Since all atoms at the As/Si interfaces are fully coordinated we expect that the dielectric model is not an unreasonable one, despite the lack of spherical symmetry. Inserting values for k and dk/dN into Eq. (9), we obtain for Si

$$\Delta\xi_{\text{Si}} = -3.28\Delta q_{\text{Si}} - 18.07\Delta(1/\epsilon_{\text{Si}}), \quad (10)$$

and for As,

$$\Delta\xi_{\text{As}} = -2.83\Delta q_{\text{As}} - 16.83\Delta(1/\epsilon_{\text{As}}). \quad (11)$$

Equations (10) and (11) give two equations in four unknowns, namely, Δq and $\Delta(1/\epsilon)$ for each element. The imposition of charge conservation across the interfaces ($\Delta q_{\text{As}} = -\Delta q_{\text{Si}}$) reduces the problem to two equations in three unknowns.

The dielectric constant of bulk Si is 12 and bulk As, as a semimetal, can be assumed to have $\epsilon \sim \infty$. In order to determine the extent of charge transfer across As/Si interfaces it is necessary to make sensible assumptions concerning the screening efficiency of core holes for As and Si atoms at the interfaces. In the language of Eq. (11), this amounts to ascribing appropriate effective dielectric constants for the interface layers. Since dielectric response is essentially determined by the amount of mobile charge, and this may be different at bulk and interface sites, we assume that the local dielectric properties at the interface may be described in terms of a “local effective dielectric constant” $\epsilon_{\text{interface}}^Z$, where Z can be As or Si. One may expect *a priori* that the effective dielectric constants at the As and Si atoms at As/Si interfaces have values between those of the respective elemental solids.

1. Simple screening models

Equations (10) and (11) impose quite powerful constraints on the value of the screening contributions to the environmental dependence of the elemental Auger parameters. This can be seen by considering several simple screening models. If we assume an “unperturbed” model in which the screening at the As and Si interface sites is the same as in the respective elemental solids, i.e., $\Delta(1/\epsilon) = 0$ for both As and Si atoms, we obtain charge distributions at the two interfaces given by $\text{Si}^{-0.15}\text{As}^{+0.2}$ for As/Si(100) and $\text{Si}^{-0.0}\text{As}^{+0.35}$ for As/Si(111), results which are not compatible with charge conservation. Similar problems are encountered using other extreme screening assumptions. For example, if the interface As and Si layers are assumed to be metallic in nature, i.e., $\epsilon \sim \infty$, we obtain $\text{Si}^{+0.3}\text{As}^{+0.2}$ for As/Si(100) and $\text{Si}^{+0.4}\text{As}^{+0.35}$ for As/Si(111), while if it is assumed that the interface layers are screened as in bulk Si we find $\text{Si}^{-0.15}\text{As}^{-0.3}$ for As/Si(100) and $\text{Si}^{-0.0}\text{As}^{-0.15}$ for As/Si(111). These results are clearly unsatisfactory and demonstrate the sensitivity of the final state AP shifts to the interface dielectric properties, and hence the need for a more realistic treatment of the screening at the interfaces.

2. “Mean effective” screening

We now adopt the assumption that the As and Si interface layers have the same effective screening environ-

ment, i.e., $\epsilon_{\text{interface}}^{\text{As}} = \epsilon_{\text{interface}}^{\text{Si}} (= \epsilon_{\text{interface}})$ — the “mean effective” screening model. Denoting the mean effective dielectric constant of the As/Si(100) and As/Si(111) interfaces by ϵ_{100} and ϵ_{111} , respectively, Eqs. (10) and (11) become

$$\Delta\xi_{100}^{\text{Si}} = -3.28\Delta q_{100}^{\text{Si}} - 18.07 \left(\frac{1}{\epsilon_{100}} - \frac{1}{\epsilon_{\text{Si}}} \right), \quad (12)$$

$$\Delta\xi_{100}^{\text{As}} = -2.83\Delta q_{100}^{\text{As}} - 16.83 \frac{1}{\epsilon_{100}}, \quad (13)$$

with corresponding equations in $\Delta\xi_{111}$, Δq_{111} , and ϵ_{111} . Imposing the constraint of charge conservation at the interface, Eqs. (12) and (13) can be solved for ϵ_{100} and Δq_{100} . At the As/Si(100)-(2×1) interface we find a transfer of 0.05 electrons per atom from Si to As and a mean effective dielectric constant $\epsilon_{100} = 22$. For the As/Si(111)-(1×1) interface we find $\epsilon_{111} = 15$ and a charge transfer of 0.07 electrons per atom from Si to As. As expected, the mean effective dielectric constant at the interface in both systems is found to be between the values of bulk Si and As.

It should be noted that experimental errors in measuring $\Delta\xi$ correspond to $\sim 15\%$ uncertainty in Δq and $\sim 3\%$ uncertainty in $\epsilon_{\text{interface}}$ in these systems.

3. “Differential” screening

In reality, one expects on the basis of the availability of screening charge that the mean effective model is an exaggeration and that the As atoms at the interface are better screened than the atoms in the Si interface layer, i.e.,

$$\epsilon^{\text{As}} > \epsilon_{\text{interface}}^{\text{As}} > \epsilon_{\text{interface}} > \epsilon_{\text{interface}}^{\text{Si}} > \epsilon^{\text{Si}}. \quad (14)$$

Thus the physical situation lies between the “unperturbed” and “mean effective” screening models. Gener-

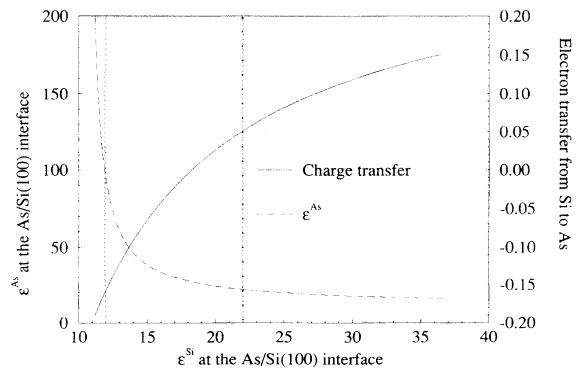


FIG. 4. Solution of Eqs. (15) and (16), the differential screening model for As/Si(100). The dielectric constant of the As overlayer $\epsilon_{100}^{\text{As}}$ (dashed curve) and the charge transfer Δq_{100} (solid curve) are plotted as functions of $\epsilon_{100}^{\text{Si}}$, the dielectric constant of the Si interface layer. The dotted vertical lines indicate the range of $\epsilon_{100}^{\text{Si}}$ permitted by the differential screening model.

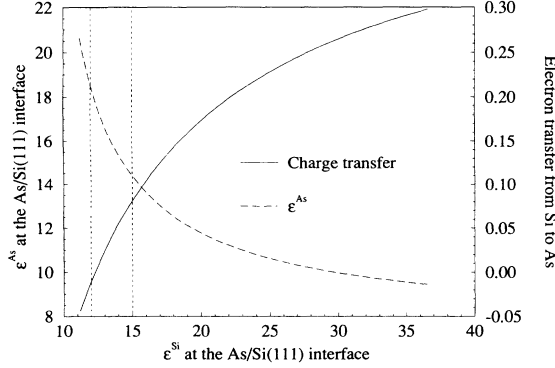


FIG. 5. Solution of Eqs. (17) and (18), the differential screening model for As/Si(111). The dielectric constant of the As overlayer $\epsilon_{111}^{\text{As}}$ (dashed curve) and the charge transfer Δq_{111} (solid curve) are plotted as functions of $\epsilon_{111}^{\text{Si}}$, the dielectric constant of the Si interface layer. The dotted vertical lines indicate the range of $\epsilon_{111}^{\text{Si}}$ permitted by the differential screening model.

alizing Eqs. (12) and (13) to allow for differential screening, and again imposing charge conservation, we obtain the relations

$$1.71 = 19.5/\epsilon_{100}^{\text{As}} + 18.1/\epsilon_{100}^{\text{Si}}, \quad (15)$$

$$0.99 = 3.28\Delta q_{100}^{\text{Si}} + 18.1/\epsilon_{100}^{\text{Si}}. \quad (16)$$

The solution set $\epsilon_{100}^{\text{As}}$ vs $\epsilon_{100}^{\text{Si}}$ is given by the dashed line in Fig. 4, while the solid curve indicates the corresponding charge transfer as a function of $\epsilon_{100}^{\text{Si}}$. Taking the condition $\epsilon_{100} > \epsilon_{100}^{\text{Si}} > \epsilon^{\text{Si}}$ (delimited in Fig. 4 by the vertical dotted lines), we find that $\epsilon_{100} < \epsilon_{100}^{\text{As}} < 100$, and the charge transfer from Si to As is constrained by $-0.15 < \Delta q < 0.05$.

Solution of the differential screening model for the As/Si(111) system is shown in Fig. 5. The effective dielectric constants and the charge transfer at the interface are related by

$$2.56 = 19.5/\epsilon_{111}^{\text{As}} + 18.1/\epsilon_{111}^{\text{Si}}, \quad (17)$$

$$1.47 = 3.28\Delta q_{111}^{\text{Si}} + 18.1/\epsilon_{111}^{\text{Si}}. \quad (18)$$

If we use the relation $\epsilon_{111} > \epsilon_{111}^{\text{Si}} > \epsilon^{\text{Si}}$ indicated by the vertical lines in Fig. 5, we find that $\epsilon_{111} < \epsilon_{111}^{\text{As}} < 20$ and the charge transfer from the Si to the As across the interface is less than 0.07 electrons per atom.

VI. CHARGE TRANSFER AND SCREENING EFFICIENCY AT As TERMINATED Si SURFACES

A. Charge transfer

Analysis of the initial state AP shifts for As and Si atoms at As terminated Si(100) and Si(111) surfaces rel-

ative to their bulk values indicates electron transfer from Si to As across the interfaces in both systems. Quantitative estimates of the charge transfer consistent with charge conservation and with the known screening properties of the bulk elemental solids deduced from the observed final state shifts $\Delta\xi$ confirm this. The mean effective screening approach suggests a transfer of ~ 0.05 electrons per atom from Si to As in both systems, consistent with the greater electronegativity of As. Although we expect the mean effective dielectric constants $\epsilon_{\text{interface}}$ to be indicative of both As and Si interface screening environments, adopting the more realistic differential screening model in which core holes on As sites are better screened than on interface Si sites (i.e., allowing the divergence of $\epsilon_{\text{interface}}^{\text{As}}$ and $\epsilon_{\text{interface}}^{\text{Si}}$ from $\epsilon_{\text{interface}}$), we find that the charge transfer estimates are reduced. We therefore conclude that ~ 0.05 electrons per atom is an upper bound on the ground state electron transfer from Si to As across the As/Si(100) and As/Si(111) interfaces.

B. Core hole screening efficiency

In terms of the mean effective screening model, we find that

$$\epsilon^{\text{Si}} \lesssim \epsilon_{111} < \epsilon_{100} < \epsilon^{\text{As}}. \quad (19)$$

In other words, the core hole screening efficiency at the As/Si(100) interface is much better than at the As/Si(111) interface. This can be clearly seen in Figs. 4 and 5. Even given the spread of values of $\epsilon_{\text{interface}}^{\text{Si}}$ and $\epsilon_{\text{interface}}^{\text{As}}$ permitted by the differential screening model, the As/Si(100) system clearly has the more favorable screening environment.

We also note that $\epsilon_{111} \sim \epsilon^{\text{Si}}$, and the differential screening approach allows little divergence of $\epsilon_{111}^{\text{Si}}$ and $\epsilon_{111}^{\text{As}}$ from ϵ_{111} . This result implies that As termination of the Si(111) surface gives an almost bulk-Si-like screening environment at the surface. This seems wholly reasonable since As terminates the Si(111) surface giving an unreconstructed bulk terminated surface geometry. The tetrahedral bonding is preserved with each As atom bonding to three interface Si atoms and the As lone pairs replacing the Si-Si bonds in the $\langle 111 \rangle$ direction. Although As-Si bonds may be expected to be more polarizable than Si-Si bonds, the screening environment of the Si interface atoms is not significantly improved with respect to a bulk lattice site.

At the 2×1 reconstructed As terminated Si(100) surface, one may expect the As dimers to form an effective screening reservoir. We may then attribute the fact that our results indicate a better screening environment at the As/Si(100) interface to the formation of readily polarizable As-As dimer bonds.

VII. CONCLUSIONS

Initial state and final state Auger parameters of As and Si for As terminated Si(100) and Si(111) surfaces

have been measured and related to the charge transfer and the screening properties at the interfaces. Estimates of charge transfer based on initial state AP shifts indicate electron transfer from Si to As in both systems. Analysis of final state AP shifts confirms this, but suggests that the charge transfer is small (~ 0.05 electrons per atom). The improved screening environment at the As/Si(100)-(2 \times 1) surface indicated by the final state AP shifts is attributed to the formation of polarizable As-As dimer bonds. The almost bulk-Si-like screening environment at the As/Si(111)-(1 \times 1) surface is consistent with the tetrahedral surface structure.

We point out that interpretation of XPS shifts alone may give a very misleading picture of the charge transfer at interfaces. AP analysis, on the other hand, allows the separation of ground state and relaxation energy shifts.

The measurement of AP shifts provides a local probe of surfaces and interfaces, and the present study indicates the wealth of electronic structure information they can supply. An understanding of the charge transfer and dielectric properties of semiconductor interface layers is relevant to device fabrication and performance. AP analysis of the kind presented here should prove useful in this area.

ACKNOWLEDGMENTS

The authors wish to thank Catherine Baker for her assistance in computing the Madelung potentials. This work was supported by the Basic Research Action of ESPRIT (Grant No. EASI; 6878) funded by the European Community.

-
- ¹ M. Copel, M. C. Reuter, E. Kaxiras, and R.M. Tromp, *Phys. Rev. Lett.* **63**, 632 (1989).
- ² M. Copel, M.C. Reuter, E. Kaxiras, H. von Hoegen, and R.M. Tromp, *Phys. Rev. B* **42**, 11 682 (1990).
- ³ M.N. Charasse and J.P. Hirtz, *Phys. World* **3** (1), 28 (1990).
- ⁴ R.D. Bringans, *Crit. Rev. Solid State Mater. Sci.* **17**, 353 (1992).
- ⁵ E. Pehlke and M. Scheffler, *Phys. Rev. Lett.* **71**, 2338 (1993).
- ⁶ J.A. Evans, A.D. Laine, P. Weightman, J.A.D. Matthew, D.A. Woolf, D.I. Westwood, and R.H. Williams, *Phys. Rev. B* **46**, 1513 (1992).
- ⁷ D.A. Woolf, D.I. Westwood, and R.H. Williams, *Semicond. Sci. Technol.* **4**, 1127 (1989); *J. Cryst. Growth* **108**, 25 (1991).
- ⁸ P. Weightman, *Phys. Scr.* **T41**, 277 (1992).
- ⁹ D.R. Penn, *J. Electron Spectrosc.* **9**, 29 (1976).
- ¹⁰ R.J. Cole, F.M. Leibsle, D.A.C. Gregory, and P. Weightman (unpublished).
- ¹¹ L. Ley, R.A. Pollack, S.P. Kowalczyk, R. McFeeley, and D.A. Shirley, *Phys. Rev. B* **8**, 641 (1973).
- ¹² W. Richter (private communication).
- ¹³ M.A. Olmstead, R.D. Bringans, R.I.G. Uhrberg, and R.Z. Bachrach, *Phys. Rev. B* **34**, 6041 (1986).
- ¹⁴ R.D. Bringans, M.A. Olmstead, R.I.G. Uhrberg, and R.Z. Bachrach, *Phys. Rev. B* **36**, 9569 (1987).
- ¹⁵ E.J. McGuire, *Phys. Rev. A* **3**, 587 (1971).
- ¹⁶ T.D. Thomas and P. Weightman, *Phys. Rev. B* **33**, 5406 (1986).
- ¹⁷ S.D. Waddington, P. Weightman, J.A.D. Matthew, and D.C. Grassie, *Phys. Rev. B* **39**, 10 239 (1989).
- ¹⁸ T. Chasse, R. Franke, P. Streubel, and A. Meisel, *Phys. Scr.* **T41**, 281 (1992).
- ¹⁹ G. Moretti, *Surf. Interf. Anal.* **16**, 159 (1990).
- ²⁰ J.A.D. Matthew, P. Weightman, and S.D. Waddington, *J. Phys. Condens. Matter* **1**, SB217 (1989).
- ²¹ J.C. Rivière, J.A. Crossley, and G. Moretti, *Surf. Interf. Anal.* **14**, 257 (1989).
- ²² R.N.S. Sodhi and R.G. Cavell, *J. Electron Spectrosc. Relat. Phenom.* **41**, 1 (1986).
- ²³ N.D. Lang and A.R. Williams, *Phys. Rev. B* **20**, 1369 (1979).